

Supplementary Methods

Cross-hybridization of expanded repeats with off-target probe sets. The CUG^{exp} RNA in HSA^{LR} mice, when converted to CAG repeats during the preparation of target cRNA, may potentially cross-hybridize with probes that contain CTG repeats. The gcRMA method minimizes this artifact by using an algorithm that suppresses outliers, so that cross-hybridization to a single (CTG)_n-containing probe would not invalidate an entire probe set (n = 11 probes per set). However, probe level analysis indicated that cross-hybridization did create false signal elevation for two probe sets. *LOC673662* was upregulated 29- and 31-fold, and *Vps37c* was upregulated 5- and 6-fold, in lines HSA^{LR}20b and HSA^{LR}41 respectively, all with nominal P values $\leq 10^{-6}$. Both of these probe sets had an unusual design feature in which probes were tiled across a short target sequence containing a CTG repeat. The CTG repeat was represented in 6 or more of the probes within the set, and the increased signal came specifically from the repeat-containing probes. Accordingly, results from *LOC673662*, and *Vps37c* were removed from the dataset. Probe level analysis for other upregulated probe sets containing probes with (CTG)_{≥2} repeats showed no further evidence for cross-hybridization.

RNA immunoprecipitation (IP) and microarray analysis. Anti-Mbnl1 antibody A2764 (3) was used to immunoprecipitate ribonucleoprotein complexes from muscle homogenates. This rabbit polyclonal antibody recognizes a C-terminal region that is not required for RNA binding (1) and is not conserved in other Mbnl family members (2). The antibody showed monospecific detection of Mbnl1 protein, as determined by immunoblot and immunofluorescence of *Mbnl1*^{-/-} vs. *Mbnl1*^{+/+} muscle (3). The efficiency of antibody A2764 for IP was > 80%, as determined by clearance of Mbnl1 protein from muscle homogenates, or by clearance of GFP from lysates prepared from COS cells expressing a GFP-Mbnl1 fusion protein (data not shown). Antibodies were affinity purified against peptide CPIISAEHLTSHKYVTQM using a SulfoLink Kit (Pierce) and then covalently attached to magnetic beads (Dynabeads Protein G, Invitrogen) using 20 mM dimethyl pimelimidate (Pierce). For IP of muscle

homogenates, mouse vastus muscle was pulverized under liquid nitrogen and homogenized in buffer [50 mM Tris pH 7.5, 100 mM NaCl, 5 mM EDTA, 0.1% NP40, 1.5 mM MgCl₂, 1 mM PMSF, 2 mM Benzamidine and 1 x Protease Arrest (Calbiochem)]. After sonication the homogenate was centrifuged at 18,000 x g for 10 min and supernatants were pre-cleared with magnetic beads blocked with yeast tRNA (2 mg/50 ul beads). The pre-cleared supernatant was incubated with antibody-charged magnetic beads for 1 hour at 4°C and then beads were washed 4 times with 1x PBS plus 0.05% Tween-20. RNA was extracted with Tri-reagent, treated with DNase, and then amplified with Ribo-SPIA kits (NuGEN). cDNA was fragmented and labeled with biotin for hybridization to Affymetrix U430 2.0 microarrays. Analysis was performed on duplicate IP samples from WT mice. Duplicate IPs from *Mbnl1*^{-/-} mice served as control for non-specific pull down. For WT IP samples the signal values for duplicate unscaled arrays were highly concordant (correlation coefficient = 0.98 and mean signal values for detected transcripts were 141 and 162, respectively). These arrays were not normalized further. For *Mbnl1*^{-/-} IP samples the duplicate arrays were less concordant (correlation coefficient = 0.95 and mean signal values for detected transcripts were 76 and 30). These samples were scaled to produce equivalent signal intensity across both *Mbnl1*^{-/-}-IP arrays. To identify Mbnl1-interacting mRNAs whose expression was altered in Mbnl1 knockout mice we examined the intersection of two datasets:

A. Transcripts highly enriched in the anti-Mbnl1 IP (n = 847). Transcripts were considered highly enriched in the IP if three conditions were met: (1) the transcript was detected in both WT-IP samples (probability of detection < 0.1 on both WT-IP arrays); (2) the mean signal was > 50-fold greater in WT-IP than in *Mbnl1*^{-/-}-IP; and (3) pairwise comparison of each WT-IP vs. each *Mbnl1*^{-/-}-IP showed > 25-fold enrichment in the WT-IP.

B. Transcripts dysregulated in Mbnl1 knockout mice in a myotonia-independent fashion (n = 733). This dataset included transcripts that showed (1) differential expression in *Mbnl1*^{-/-} vs. *Mbnl1*^{+/+} muscle (fold-change > 1.5, nominal *P* < 0.01); and (2) no change in the same direction in *Clcn1*^{-/-} vs. WT mice (nominal *P* > 0.05).

The intersection of these datasets contained 52 transcripts, of which 48 (92%) were downregulated in *Mbn1^{-/-}* muscle. As most of these transcripts have reduced abundance in *Mbn1^{-/-}* muscle, some enrichment in WT vs. *Mbn1^{-/-}* IP could result from lower concentration in the *Mbn1^{-/-}* input. However, two observations indicate that this is unlikely to explain strong enrichment that was observed in the WT IP with respect to the *Mbn1^{-/-}* IP:

1. The fold-enrichment of the 52 transcripts in the WT vs. *Mbn1^{-/-}* IP (mean enrichment 213-fold, range 50- to 932-fold) was much greater than the extent of their reduction in *Mbn1^{-/-}* input (mean reduction in *Mbn1^{-/-}* vs. WT total cellular RNA was -2.1-fold, range -1.5 to -8.2-fold).
2. We used a second metric to verify enrichment of these 52 transcripts in the anti-Mbn1 IP, without reference to *Mbn1^{-/-}* mice. This analysis was based on the rank order of microarray signal intensity in WT mice. We first selected all probe sets that showed detectable signal in WT total cellular RNA (n = 22,917). We then ordered these probe sets from lowest to highest signal intensity using signal from arrays hybridized with total cellular RNA. We repeated this procedure using signal from arrays hybridized with IP RNA. An upward shift in the signal rank in IP as compared to total cellular RNA was taken as evidence for enrichment in the IP. The 52 transcripts uniformly showed an upward rank shift in the IP RNA (mean upward shift by +5,312 ranks, range +521 to +12,951 ranks), consistent with enrichment in the anti-Mbn1 IP. By comparison, the mean shift across all muscle-expressed genes was 0.

Pathway analysis. Pathway analysis was carried out using Ingenuity Pathways Analysis (4) (IPA, www.ingenuity.com), Gene Set Enrichment Analysis (5) (GSEA, www.broad.mit.edu/gsea/), and Expression Analysis Systematic Explorer (6) (EASE). IPA uses a curated library of gene sets to identify canonical pathways that show coordinate dysregulation (4). Genes that met threshold criteria of > 2 fold-change and nominal $P < 0.01$ for the mutant vs. WT comparison were included in the analysis. The significance of the association between the dataset and a canonical pathway was measured in two ways: 1) a ratio of the number of genes passing the threshold cutoff that map to the pathway divided by the

total number of genes in the canonical pathway; and 2) Fischer's exact test to estimate the probability that association between genes in the dataset and a canonical pathway is explained by chance alone. GSEA tests for similar changes in expression among multiple related genes, where relatedness is operationally defined by known biochemical function, co-regulation in previous expression profile experiments, or similarity of transcription factor binding domains in promoter regions (5). The details of the gene sets examined with GSEA are listed in the Molecular Signatures Database (www.broad.mit.edu/gsea/msigdb/). This method does not impose any threshold criteria for altered expression. Rather, it estimates the likelihood that changes in expression of a particular pathway or gene set may occur by chance alone. The EASE method was used to compare lists of differentially expressed genes to the entire list of expressed genes to determine if certain Gene Ontology categories were over-represented (6). Use of strict criteria to define differential expression limits the utility of this approach, so we included all effects with nominal $P < 0.01$, with no fold-difference criterion. Pathways with an EASE score < 0.001 were considered to show dysregulation.

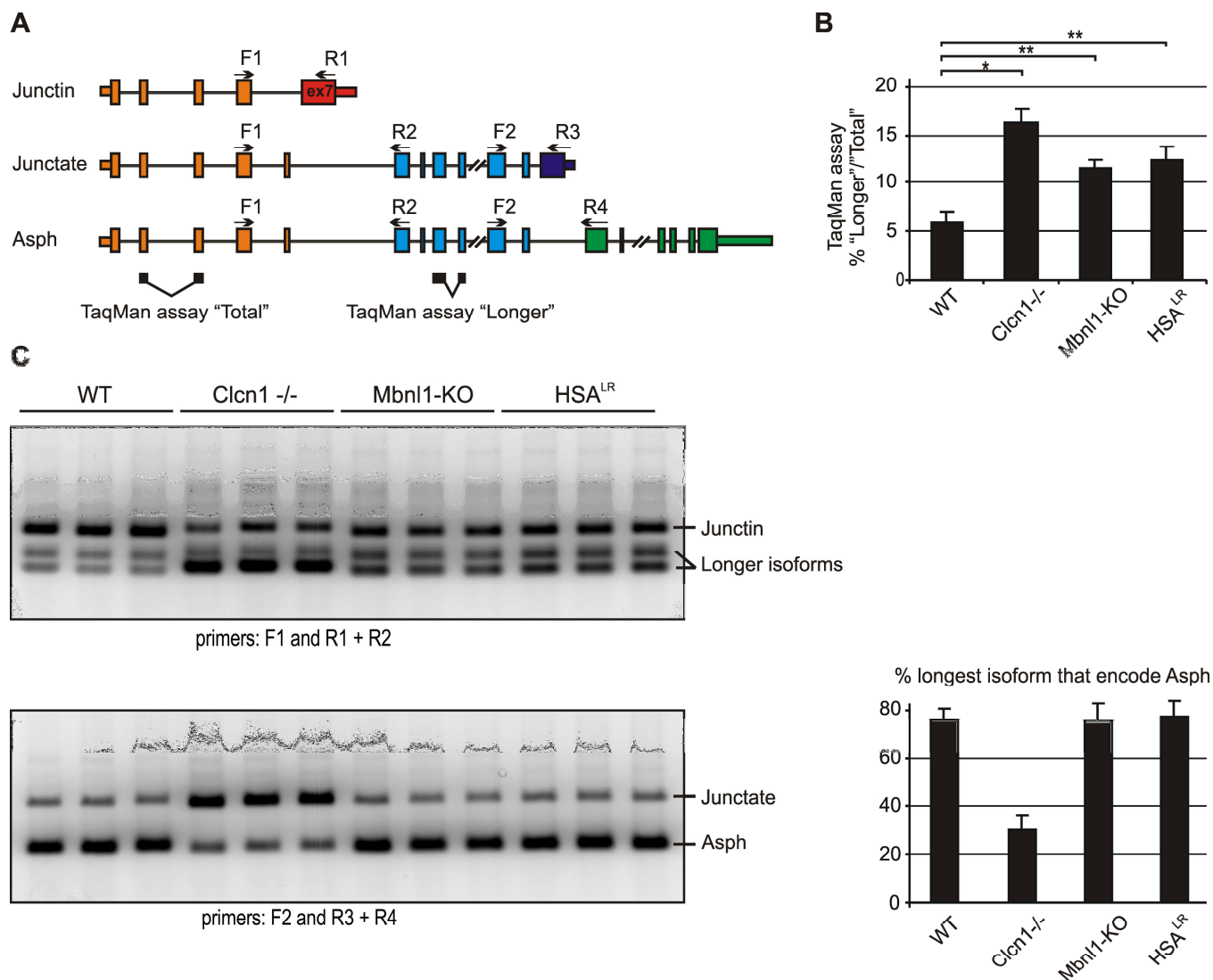
Primer sequences.

Gene	Forward	Reverse
Primers for RT-PCR		
<i>HSA^{LR}</i>	5'-ACACACTCCACCTCCAGCA-3'	5'-TAAACACTGTGTCAGTTTAC-3'
<i>Asph F1</i>	5'-AAGAGGAGGGATTTTCAGGAGGGTC-3'	
<i>Asph R1</i>		5'-AGCGGATGCTTTCTGGGATGTGTC-3'
<i>Asph R2</i>		5'-TCCAGCTCAGCGTGAGTCTCTG-3'
<i>Asph F2</i>	5'-GCAGTGACAGATGCAGGTGTGCTG-3'	
<i>Asph R3</i>		5'-AACCCAACTGAGCCACAGATGCTC-3'
<i>Asph R4</i>		5'-ACCCCTTTTCCGGAGCTTTTCTGC-3'
Primers for competitive RT-PCR of mRNA		
<i>Sln</i>	5'-CAGGAAGTGAAGACAAGCCTTG-3'	5'-CACACAGCAGTCACTCCCTG-3'
<i>Myo1A</i>	5'-GGACATCCTGCTAGTGAGCGAC-3'	5'-GCCCTGGATAACCTTGACAGC-3'
<i>Uchl1</i>	5'-AGGGCCAGTGTCTGGGTAGATG-3'	5'-GCTCGCGCTCAGTGAATTCTC-3'
<i>Cpne2</i>	5'-CCACTAACCCTTTCTGCTCAG-3'	5'-CCTCCATGTCCTGATGACC-3'
<i>Xedar</i>	5'-ATGTGTCTGAGCCAAGTTTAG-3'	5'-CTTGAGATTGAAGCATTGCC-3'
<i>Casp12</i>	5'-GACCCAGATGCCACTATTG-3'	5'-TTTGGGAAGGAAGGAACGAATC-3'
<i>Kcnab1</i>	5'-TGGTGCCATTCAGGTCCTCC-3'	5'-TGCACAGTGGTAGCAACAGCAG-3'
<i>Myo15</i>	5'-ATCCTCGCTGTCAACCATAACG-3'	5'-TAGGCCACGTCACAAGAGGG-3'
** <i>Cpne2</i>	5'-GAAATGACTCCAGCAGAAC-3'	5'-AGGCAGATGCCAATATTTATAC-3'
** <i>Xedar</i>	5'-CTGCCAGGAACTGTTGCTG-3'	5'-TCCGCCAACACCGCTTTAG-3'
Primers for competitive RT-PCR of pre-mRNA		
<i>Sln</i>	5'-CAAACACATGAATCTCTGG-3'	5'-GCTTGTCTTCACTTCCTAAC-3'
<i>Xedar</i>	5'-TTGGTGTCTGTTTGTGTGGTAG-3'	5'-GAGAGAACATGGTTGCCTATTG-3'
<i>Kcnab1</i>	5'-AAGGCACTGGTGGGCATTCC-3'	5'-ATGCTGGACAAGGAAAGCCTTC-3'
<i>Uchl1</i>	5'-CGGGAGAAATAAGGCTGACCC-3'	5'-AGCACAAAGCTCAGCCACAC-3'
Primer used to generate internal competitive standard		
<i>Sln</i>	5'-CAAACACATGAATCTCTGGAAGTTGATGCTGAAGCTACC-3'	
<i>Xedar</i>	5'-TTGGTGTCTGTTTGTGTGGTAGATAAGTAGATGTGGCCCC-3'	
<i>Kcnab1</i>	5'-AAGGCACTGGTGGGCATTCCCTGGTGATAATATATTGCTT-3'	
<i>Uchl1</i>	5'-CGGGAGAAATAAGGCTGACCCAGTCTCTGTCCCTATCCTC-3'	

References

1. Yuan, Y., Compton, S.A., Sobczak, K., Stenberg, M.G., Thornton, C.A., Griffith, J.D. and Swanson, M.S. (2007) Muscleblind-like 1 interacts with RNA hairpins in splicing target and pathogenic RNAs. *Nucleic Acids Res*, **35**, 5474-86.

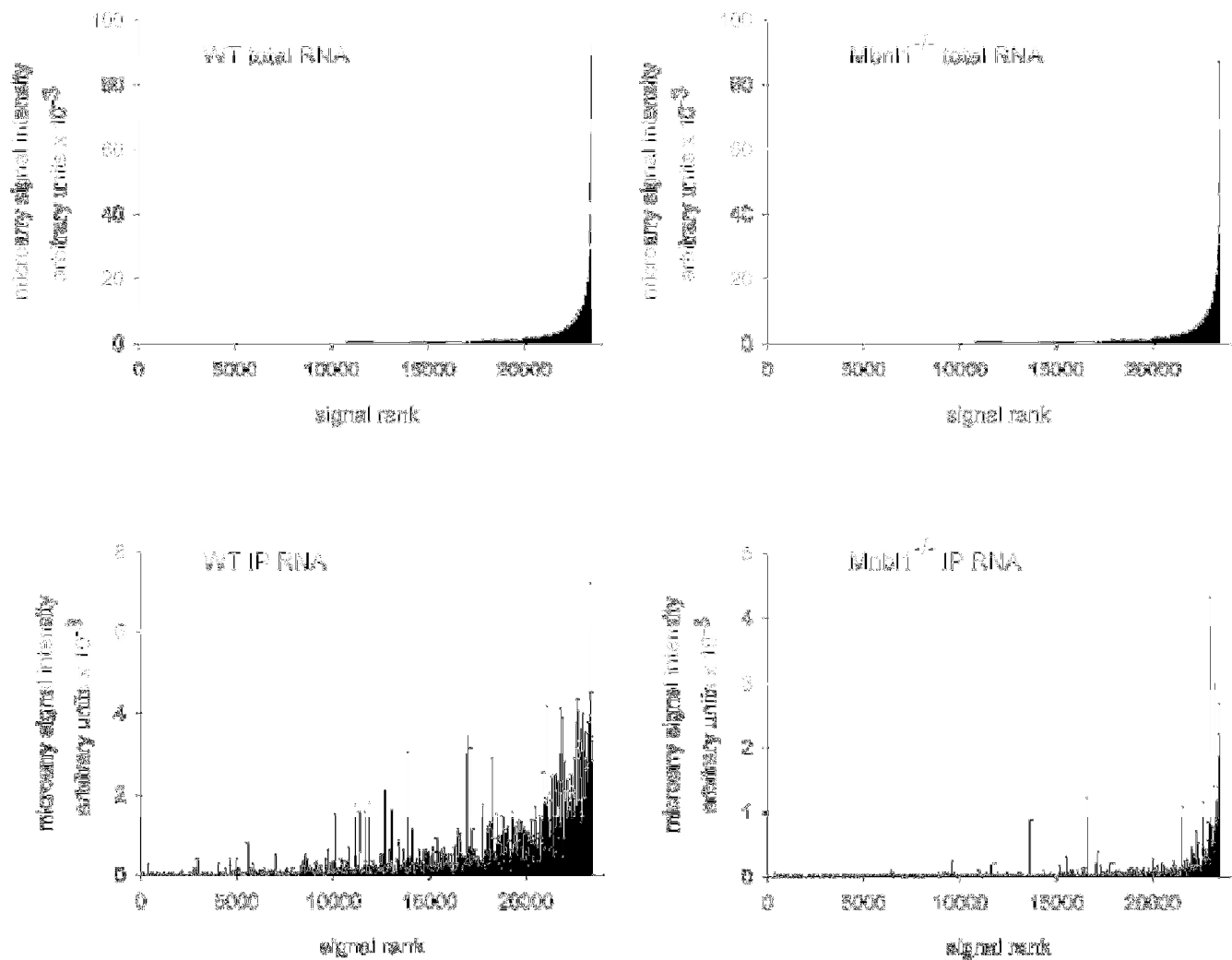
2. Farfardai, M., Rogers, M.T., Thorpe, H.M., Larkin, K., Hamshere, M.G., Harper, P.S. and Brook, J.D. (2002) Three proteins, MBNL, MBLL and MBXL, co-localize in vivo with nuclear foci of expanded-repeat transcripts in DM1 and DM2 cells. *Human Molecular Genetics*, **11**, 805-814.
3. Lin, X., Miller, J.W., Mankodi, A., Kanadia, R.N., Yuan, Y., Moxley, R.T., Swanson, M.S. and Thornton, C.A. (2006) Failure of MBNL1-dependent postnatal splicing transitions in myotonic dystrophy. *Human Molecular Genetics*.
4. Calvano, S.E., Xiao, W., Richards, D.R., Felciano, R.M., Baker, H.V., Cho, R.J., Chen, R.O., Brownstein, B.H., Cobb, J.P., Tschoeke, S.K. *et al.* (2005) A network-based analysis of systemic inflammation in humans. *Nature*, **437**, 1032-1037.
5. Subramanian, A., Tamayo, P., Mootha, V.K., Mukherjee, S., Ebert, B.L., Gillette, M.A., Paulovich, A., Pomeroy, S.L., Golub, T.R., Lander, E.S. *et al.* (2005) Gene set enrichment analysis: a knowledge-based approach for interpreting genome-wide expression profiles. *Proc.Natl.Acad.Sci.U.S.A*, **102**, 15545-15550.
6. Hosack, D.A., Dennis, G., Jr., Sherman, B.T., Lane, H.C. and Lempicki, R.A. (2003) Identifying biological themes within lists of genes with EASE. *Genome Biol.*, **4**, R70.



Supplementary Figure 1. DM1 models and *Clcn1* null mice display differential expression of *Asph* isoforms with alternative 3' ends.

(A) Alternative splicing of *Asph* generates transcripts with different 3' ends, encoding proteins that are functionally distinct (reviewed in (1)). The shortest isoform, which predominates in skeletal muscle, encodes junctin, the intermediate isoform encodes junctate, and the longest isoform encodes aspartate beta hydroxylase. Junctin and junctate have a role in Ca^{2+} homeostasis in the sarcoplasmic reticulum (1). "Total" denotes qRT-PCR primers that amplify all *Asph* splice products. "Longer" denotes qRT-PCR primers that amplify junctate or aspartate beta hydroxylase mRNA. Microarray data (not shown) indicated upregulation of aspartate beta hydroxylase mRNA in *HSA*^{LR} and *Mbnl1* knockout mice, and of junctate mRNA in *Clcn1* null mice. (B) qRT-PCR indicated that total levels of

Asph expression are unchanged, and verified that DM1 models and *Clcn1* null mice have upregulation of “longer” isoforms ($n \geq 3$ per group; * denotes $P < 0.0001$, ** denotes $P < 0.001$; *t*-test), consistent with a myotonia-induced increase of exon 7-skipped (shown in red in **A**) splice products. (**C**) RT-PCR analysis of *Asph* splice products. To test for differences in the ratio of splice products containing alternative 3' ends, the assays contain three primers (one forward, two reverse, with one reverse primer positioned in the alternative 3' end-exon). The upper panel shows analysis of 3' ends comprised of exon 7, and confirms increased exon 7-skipped splice products in *Clcn1* null, *Mbn1* knockout, and *HSA*^{LR} mice. Note that “longer isoforms” are represented by a doublet, owing to alternative splicing of an internal exon cassette. The lower panel shows that *Clcn1* null mice, but not *Mbn1* knockout or *HSA*^{LR} mice, have increased utilization of the 3' end-exon that encodes junctate. Comparison of *Clcn1* null with *Clcn1*^{+/+} littermates confirms that this difference does not result from strain background (not shown). Thus, consistent with microarray data, *Clcn1* null mice have upregulation of junctate, whereas DM1 models have upregulation of aspartate beta hydroxylase. Bar graph shows mean \pm S.D for $n = 6$ samples per group ($P < 0.0001$).



Supplementary Figure 2. Distribution by rank of probe set signal intensities. All probe sets that showed detectable gene expression in total cellular RNA from WT (left) or Mbn1 knockout (right) muscle were ranked according to signal intensity (upper panels). The same order of probe sets was used to display signal intensities for RNAs that co-immunoprecipitate with anti-Mbn1 antibodies (lower panels). For Mbn1 knockout mice, the distribution of the IP'ed RNA generally conforms with total cellular RNA, and mainly consists of non-specific pull down of high abundance transcripts. By contrast, the distribution of co-IP RNA from WT mice is much broader, and includes many transcripts of low or intermediated expression level.

References

1. Hong, C.S., Kwon, S.J. and Kim do, H. (2007) Multiple functions of junctin and junctate, two distinct isoforms of aspartyl beta-hydroxylase. *Biochem Biophys Res Commun*, **362**, 1-4.